Optica Applicata, Vol. XLVI, No. 2, 2016
DOI: 10.5277/oa160211

Fusion splicing: the penalty of increasing the collapse length of the air holes in ESM-12B photonic crystal fibers

SALAH A. ADNAN[1], AHMED W. ABDULWAHHAB[1], SHAYMAA N. ISMAIL[2]

[1]Department of Laser and Optoelectronics Engineering, University of Technology, Baghdad, Iraq

[2]Department of Applied Science, University of Technology, Baghdad, Iraq

For optimum fusion splicing process of a photonic crystal fiber, the collapsing of the air holes at any photonic crystal fiber is the key point of either increasing or decreasing the total splice loss. In this paper, an experimental study has been carried out to investigate the relation between total splice loss or total fiber attenuation due to splice loss and the length of the collapsed region of the air holes. This is done by splicing ESM-12B photonic crystal fiber between two equal lengths of single mode fibers and measuring the attenuation at different arc times and arc powers. The results showed that the increase in the length of the collapsed air holes region results in higher loss, therefore, higher fiber attenuation.

Keywords: photonic crystal fiber (PCF), collapse length, mode field diameter (MFD), fusion splicing, guiding mechanisms.

1. Introduction

In the last two decades, high performance optical fiber communications and other optical devices extremely rest on the improvement of the fiber manufacturing technology. This led to finding new design approaches of fibers more suitable to specific kind of applications. Photonic crystal fibers (PCFs) emerged as a new design approach used in different applications such as fiber communication systems, fiber lasers, sensing applications and so on [1]. In contrast to conventional optical fibers, the PCF has different unique characteristics such as low dispersion, high birefringence and lower nonlinearity. All these properties have come from its unique design of running a number of air filled holes along the length of the PCF to make more endlessly single mode confinement [2]. In terms of light guiding, the PCF shows two different types of guiding mechanisms. According to the type of the PCF which can be solid core (solid core of fused silica surrounded by a periodic structure of air-holes-silica cladding) or hollow core (air-holes-silica cladding surrounding the air filled core), the light will propagate in different ways. In the solid core PCFs, the guiding mechanism is based on the principle of modified total internal reflection (TIR). However, hollow core PCFs depend

mainly on the photonic band-gap (PBG) mechanism [3]. The effective refractive index of the PCF can be considered as the most advantageous factor in studying guiding mechanisms of the PCF because it contains information of both dispersion and loss characteristics in its complex mathematical form [4]. In this paper, an experimental investigation will be carried to explore how the total fiber attenuation will be altered with respect to the length of the air holes collapsed region as a function of different fusion splicing arc times and arc powers. Moreover, a comparison between all the results will be investigated to find the most optimum arc power that can make lower effects on the air holes collapse length by taking different arc power values of STD 00 bit, STD +10 bits and STD –10 bits.

2. The challenge in splicing PCF with SMF

In any splicing operation, the key point is the mode coupling between two fibers. If there is any mismatch during the splicing process, loss will be the cost. Therefore, it is important to ensure that the efficiency of light coupling from a single mode fiber (SMF) to the PCF is as good as possible, in other words, with the high coupling efficiency. However, the challenge in splicing conventional SMFs with the PCF raises from the fact that the PCF has a periodic number of microstructure air holes surrounding the core. The process of the fusion splicing works to destroy the guiding mechanism of the PCF and then more power could be lost [5]. In a conventional SMF, the fusion splicing is accomplished by heating both ends of the fibers just above the softening point, pressing, and joining them together to make a join point. In the PCF, the principle is similar to that of the SMF, but as temperature increases above the softening point, the tension on the surface of the PCF will overcome the viscosity and the microstructure air holes will completely be collapsed resulting in more loss. The reason for this phenomenon is the fact that there is a difference in softening point temperature between both SMF and PCF, where PCF has a lower softening point than the SMF. This is raising from the smaller solid core diameter and coexistence of the air holes along the fiber [6, 7]. The following relation shows the rate of micro-air holes collapse [8, 9]:

$$V_{\text{collapse}} = \frac{\gamma}{2\eta} \tag{1}$$

where γ and η are the surface tension and viscosity, respectively. From Eq. (1), the viscosity is significantly decreasing with increasing temperature. Therefore, more holes lack their cylindrical shape and disturb the guiding mechanism in the PCF. An important point should be also noted that in the PCF with different air-hole sizes, the bigger radius will be affected by the temperature of the fusion splicing at a rate higher than the smaller radius. Further, the rate of collapse will appear on the air holes those near to the outer surface more than those at a deeper site [10]. As a result, the coupling efficiency of splicing two different types of fibers (in this case, PCF – SMF) will be reduced. The reason is back to the fact that the mode experiences more broadening at the collapsed region [11].

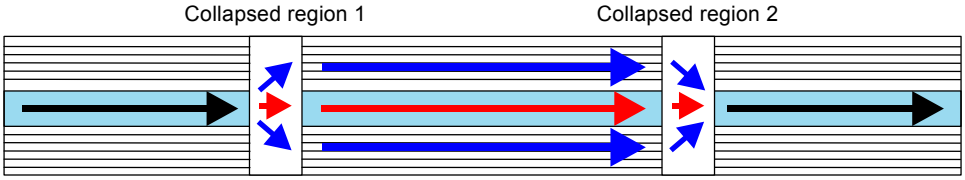

Fig. 1. The schematic of In-PCF MZI collapsing regions used to split and recombine the signals [13].

Micro-hole collapses have attained great importance in recent times due to the simple fabrication process involved and excellent sensing performance. The benefit of this physical concept of SMF-PCF-SMF splicing with the existence of a collapse region can be specifically utilized in the field of PCF Mach–Zehnder interferometer (MZI) sensing method [12]. PCF-like interferometers and assembly have been used for measuring physical, chemical, and biochemical parameters such as strain, high temperature (up to 1000°C), hydrostatic pressure, curvature, biofilm, and chemical vapor. The concept of sensing comes from the fact that the collapsed region allows the excitation of two modes in the PCF, and the length of the collapsed region is typically less than 300 or 400 µm depending on the fusion splicing parameters, the process and the type of PCF used for such application. Figure 1 shows the schematic of In-PCF MZI.

3. Experimental procedure

In this work, two equal lengths of single mode optical fibers (SMF-28) were considered as the main parts of our experiment. The specification of the SMFs used in our experiments are SMF-28 with mode field diameter (MFD) and core diameters at 1550 nm are ~10.4 and 8.2 µm, respectively [9]. The most important part is the photonic crystal fiber (ESM-12B) that comes with the following physical properties: 12.00 ± 0.5 µm core diameter, 125 ± 5 µm cladding diameter, 10.4 µm mode field diameter [14], and pure silica core and cladding materials, surrounded by air hole lattice as shown in Fig. 2, minimum loss between 700 to 1700 nm wavelength range and supports an endless single mode operation [11]. Further, a 1550 nm optical power transmitter and power meter were also used to measure the optical output power at various steps of

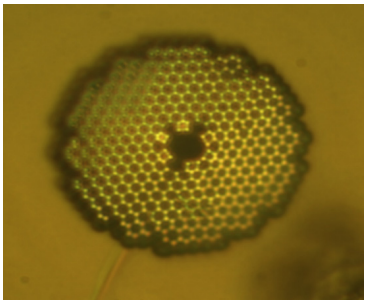

Fig. 2. Microscopic image of the solid code ESM-12B PCF.

the experiment. A very crucial step in the work is to make sure that the mode field diameters of both fibers (SMF and ESM-12B PCF) are the same but they have different core radii. In order to achieve high accuracy in stripping the coating layer and perfect longitudinal cleaving of both SMF-28 and the ESM-12B, a JIC-375 Tri-Hole stripper and CT-30 fiber optic cleaver were used respectively to ensure the best fiber preparation. Finally, the splicing process was accomplished by using a Fujikura (FSM-70s) fusion splicing machine. The measurements of the length of air holes collapsed region were performed by using a Euromex trinocular polarizing microscope model ME.2895.

3.1. Fiber preparation for splicing procedure

The experiment configuration is schematically shown in Fig. 3. It is obvious that the PCFs were spliced between two SMF-28.

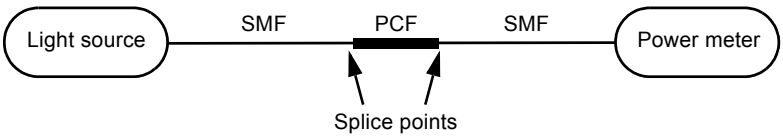

Fig. 3. Schematic configuration of the proposed experiment model.

HE -SM (HE 980-SM) modes of the fusion splicer were used for splicing. By using a trial and error method, optimum parameters of the fusion splicing have been selected to splice ESM-12 (PCF) to SMF-28 to get accurate measurement of the splice loses. The experiment setting was as follows: first, the transmission power in SMF-28 was measured by a power meter and the light source with wavelength of 1550 nm which was recorded as a reference measurement. Secondly, the SMF-28 was cleaved in the middle part. Third, the two sides of the optical fiber were stripped by a JIC-375 Tri-Hole stripper and a protective polymer coating around the optical fiber was removed. Fourth, the optical fiber was cleaved perpendicular to the longitudinal axis of the fiber. In those experiments, fiber optic cleaver (CT-30) was used. The fifth step was done by cleaning the conventional single mode fiber (SMF-28) by alcohol and tissue. The step number six was done by stripped ESM-12B using a JIC-375 Tri-Hole stripper and the protective coating around the optical fiber was completely removed. Finally, the photonic crystal fiber (ESM-12) was cleaved perpendicular to the longitudinal axis of the fiber by fiber optic cleaver (CT-30) and cleaned by a tissue only.

T a b l e 1. Pre-fuse parameters of the FSM-70s.

Splice parameters	SMF-28/PCF(ESM-12B)
Pre-fuse time	180 ms
Pre-fuse power	Standard
Overlap	10 μm
Gap	15 μm

3.2. SMF-ESM-12B PCF-SMF splicing procedure

The parameters of the fusion splicer machine (FSM-70s) were carefully adjusted to maintain optimum splicing at every time we splice PCF with SMFs as shown in Table 1.

The two cleaved ends of SMF-28 and PCF (ESM-12) were placed in the splicer type (FSM-70s) and spliced by select different fusion time with the constant value of fusion power.

The procedure for splicing SMFs-28 and ESM-12B PCF was developed by attempting more than 10 samples for best results. The splicing program of SMF-28s\ESM-12B PCF\SMF-28 was performed firstly by aligning the SMF-28s and ESM-12B PCF in V-groove of Fujikura (FSM-70s) arc fusion splicer with standard pre-fused power and 180 ns pre-fuse time to ensure no end fiber contamination or dirtiness existence. This step is very crucial to ensure strong splicing and remove the possibility of weak splicing results of PCF with SMF-28. Secondly (before continuing the splicing process) two important parameters were fixed to define the distance of the SMF-28 and ESM-12B PCF from the arc fusion splicer electrodes. The first parameter is the gap distance. In our experiments, the gap distance has been chosen to be 15 μm with a positive overlap of 10 μm to provide a simple butt-couple touch point between the end fibers with no overlap between them. The second parameter, known as the offset, has been set to be non-zero of 180 value to make sure that the collapse length of the fiber is minimum during the splicing process. All details were given in Table 1. The other side of PCF (ESM-12) and SMF-28 were placed in the splicer type (FSM-70s) and spliced by selecting the same different fusion time with the constant value of fusion power. The transmission power losses in (SMF-PCF-SMF) were measured by using 1550 nm wavelength, the loss of one splice point was calculated by using the Eq. (2). The measurement of the length of air holes collapsed region was performed by using a Euromex trinocular polarizing microscope model ME.2895 at various fusion times.

In order to explore the relation between the collapse length of the air holes with respect to the total splice loss, we used to make the splicing operation at different arc times of 500, 1000, 1500, 2000, 2500 and 3000 ms every time we changed the arc powers from STD –10 bits passing through STD 00 bits to STD +10 bits. After changing the arc power and times, the output power will be recorded and the total attenuation or total splice loss will be calculated by using the following relation [8, 15]:

$$\alpha_{\mathrm{dB}} = -10\log\left(\frac{P_{\mathrm{out}}}{P_{\mathrm{in}}}\right) \tag{2}$$

$$\alpha_{\mathrm{dB}} = -20\log\left(\frac{2\,\omega_1\,\omega_2}{\omega_1^2 + \omega_2^2}\right) \tag{3}$$

where α is the total fusion splice loss in dB, P_{out} is the output power, P_{in} is the input power, ω_1 and ω_2 are mode filed diameters of PCF and SMF, respectively. Note that the P_{in} = 278 μW and was referenced just before the splicing process.

4. Results and discussion

According to the data in the sheet in [14], it is worth to mention that the mode field diameters of both ESM-12B and SMF-28 are identical. The splice loss and the collapse length of the worked samples are illustrated in Tables 2–4. In addition, Figs. 4 to 10 show various relations between tables columns.

The splice losses were calculated by using Eq. (2). From the theoretical point of view, the splice loss must be equal to zero whenever there is a matching in the MFDs between any fibers at suitable weak arc power and short duration arc time to minimize the air hole collapse. In Fig. 4, the fusion arc power was fixed to STD –10 bits, while the arc time was varied from only 500 to 3000 ms.

The smallest loss was achieved at the minimum arc time of 500 ms and the collapse was found to be only 1.2 μm, see Fig. 5**a**. This is because of matching between MFD of both SMF and ESM-12B PCF. Behind this point, there was a significant increase

T a b l e 2. Arc power STD –10 bits.

Arc time [ms]	Output power [dBm]	Attenuation [dB]	Collapse length [μm]
500	–6.021	0.4614	1.2
1000	–11.3519	5.7923	12.75
1500	–12.1801	6.6205	13.09
2000	–12.2673	6.7077	14.5
2500	–14.2754	8.7158	16.88
3000	–16.0136	10.4540	18.07

T a b l e 3. Arc power STD 00 bit.

Arc time [ms]	Output power [dBm]	Attenuation [dB]	Collapse length [μm]
500	–7.794	2.2341	5.7
1000	–9.851	4.291	8.9
1500	–12.147	6.5871	11.8
2000	–12.926	7.3664	13.48
2500	–13.959	8.4003	14.22
3000	–14.611	9.0509	16.37

T a b l e 4. Arc power STD +10 bits.

Arc time [ms]	Output power [dBm]	Attenuation [dB]	Collapse length [μm]
500	–6.5502	0.9906	5.1
1000	–8.3387	2.7791	8.7
1500	–11.0919	5.5323	11.6
2000	–12.204	6.6445	12.9
2500	–12.3657	6.8062	13.54
3000	–12.6922	7.1326	15.9

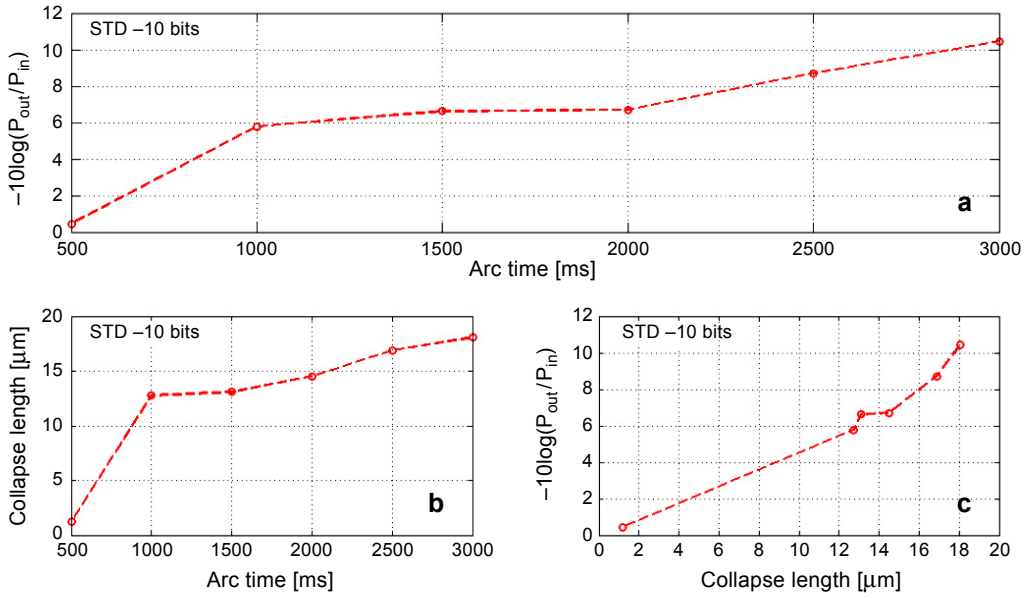

Fig. 4. Relation between different measurements at arc power of STD –10 bits: arc times *vs.* splice loss (**a**), arc times *vs*. collapse lengths (**b**), and collapse length *vs*. splice loss (**c**).

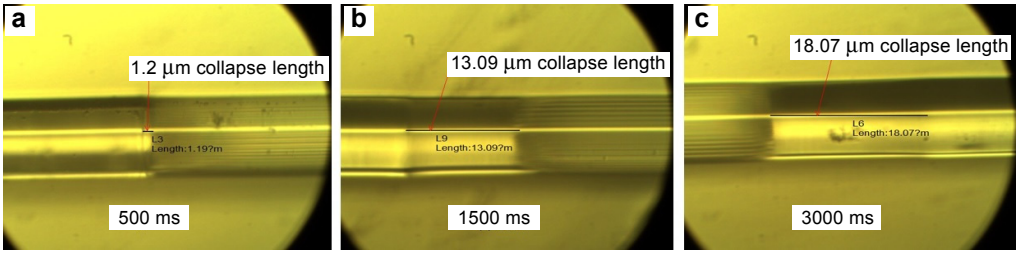

Fig. 5. STD –10 bits arc power samples of microscopic view of the spliced SMF-PCF at 500 ms (**a**), 1500 ms (**b**), and 3000 ms (**c**).

in the value of the splice loss from 0.4614 to 10.454 dB as the arc time became higher than 500 ms. This is because of the significant increase in the length of the air holes collapsed region with increasing the temperature to reach its maximum collapse length of 18.07 µm at 1500 and 3000 ms as shown in Figs. 5**b** and 5**c**, respectively. There are two reasons for increasing the splice loss with respect to the increase in arc time. Firstly, the number of the collapsed air holes. Secondly, the increase in the length of the collapsed region of the air holes with arc fusion time, that results in creating an air gap between the cores of both PCF and SMF. This will result in higher coupling loss because the outcoming light from the SMF will quickly expand in the air gap of the collapsed region [6]. Hence, the relationship between splice losses and collapse lengths is linear as in Fig. 4.

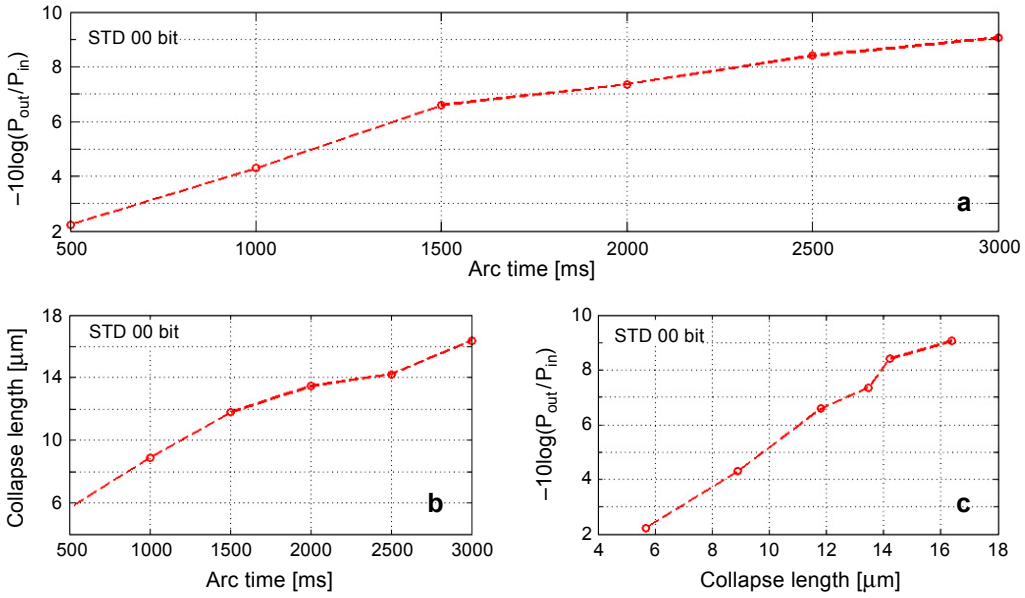

Fig. 6. Relation between different measurements at arc power of STD 00 bit: arc times *vs*. splice loss (**a**), arc times *vs*. collapse lengths (**b**), and collapse length *vs*. splice loss (**c**).

The arc fusion power was adjusted to STD 00 bit and the time was varied similar to the first case. The minimum splice loss was found to be 2.2341 dB due to 5.7 µm collapse length at 500 ms of arc time as shown in Fig. 6.

Similar to the first case, the splice losses were also increased to achieve its maximum value of 9.0509 dB at 3000 ms where the collapse length reached its maximum length of 16.37 µm. As in case of arc power STD –10 bits, the splice losses increased due to the same reasons, so that the relationship between splices losses and collapse length is almost linear as illustrated in Fig. 6**c**. The corresponding splice losses at Fig. 6**a** are shown as air holes collapse length in Fig. 7.

Moving forward and similarly to the above cases and at arc power of STD +10 bits, the smallest loss of 0.9906 dB was achieved at the minimum arc time of 500 ms due

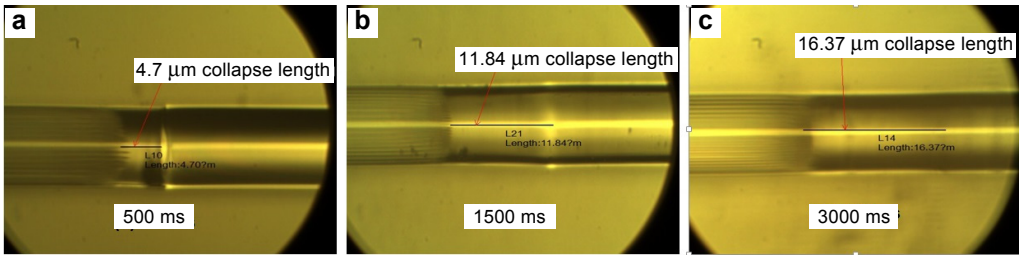

Fig. 7. STD 00 bit arc power samples of microscopic view of the spliced SMF-PCF at 500 ms (**a**), 1500 ms (**b**), and 3000 ms (**c**).

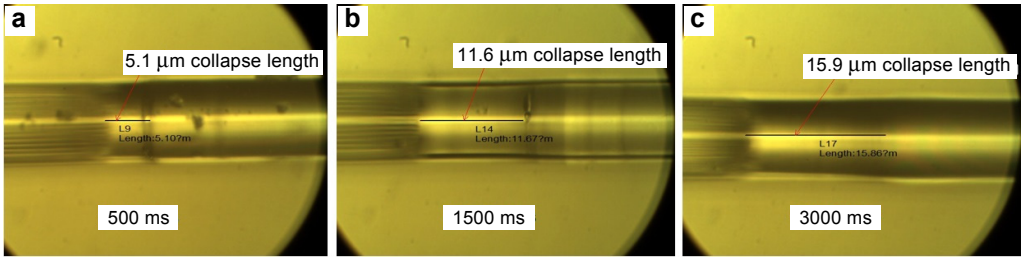

Fig. 8. STD +10 bits arc power samples of microscopic view of the spliced SMF-PCF at 500 ms (**a**), 1500 ms (**b**), and 3000 ms (**c**).

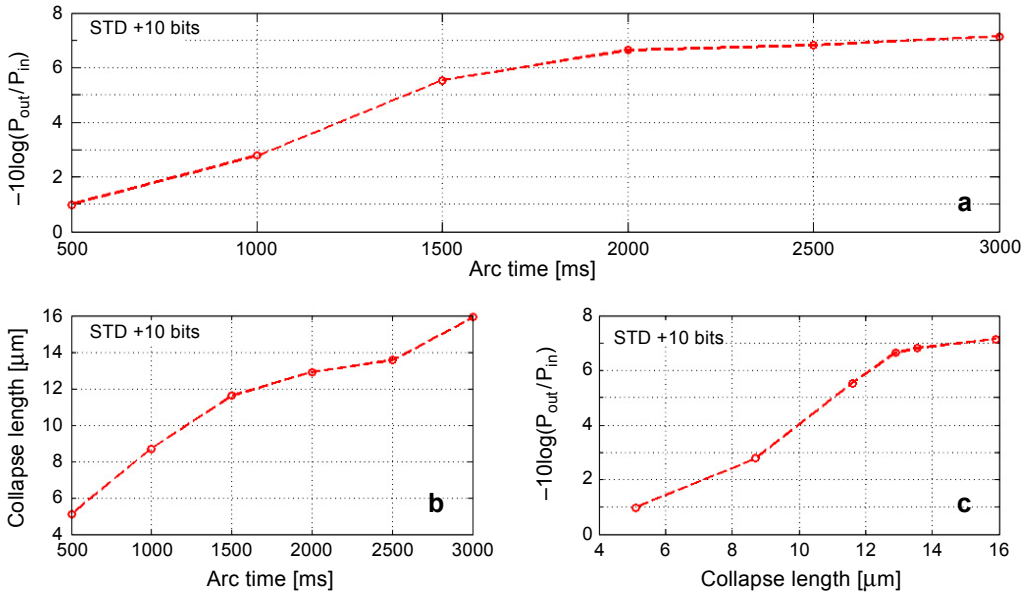

Fig. 9. Relation between different measurements at arc power of STD +10 bits arc times *vs*. splice loss (**a**), arc times *vs*. collapse lengths (**b**), and collapse length *vs*. splice loss (**c**).

to the minimum collapse length of 5.1 µm as shown in Fig. 8**a**. The corresponding collapse length and related figures for splice losses are shown in Figs. 8 and 9, respectively.

Comparatively, Fig. 10 shows the difference in splice losses of different arc fusion powers.

It is obvious that the optimum arc power that mostly resulted in lower splice loss was achieved at STD +10 bits. However, both cases of STD 00 and STD –10 bits had higher splice loss. In general, the softening point of the PCF is lower compared with the softening point of the SMF-28. At STD –10 bits, on the one hand, the PCF has reached the softening point earlier than SMF. This led to the mode filed mismatch between the PCF and SMF and the total loss was due to the collapse of the air holes and

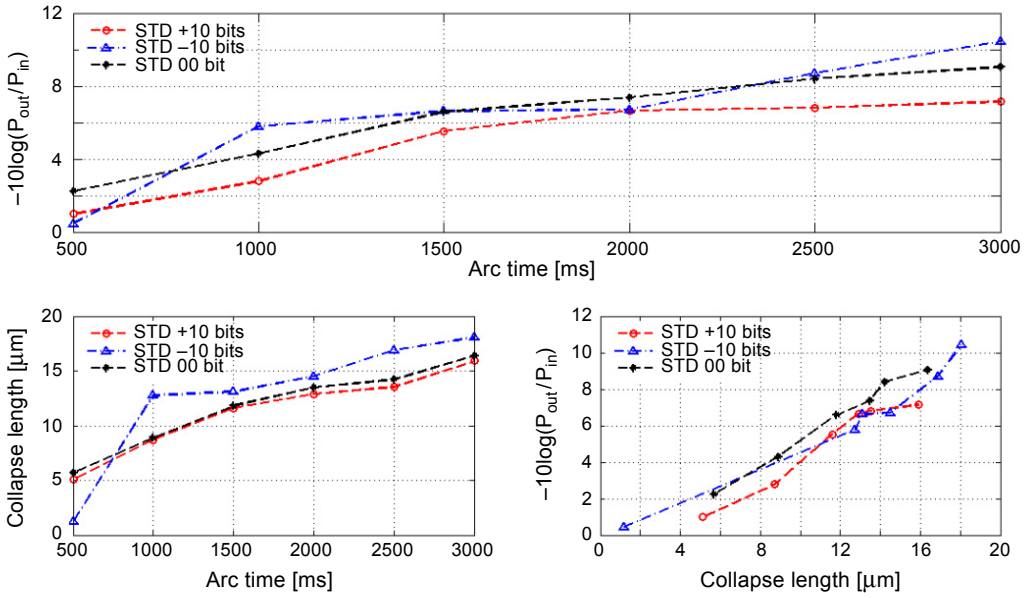

Fig. 10. Results comparison between different losses for different arc powers.

the mismatch between MFDs of different spliced fibers. On the other hand, and with arc powers of STD 00 and STD +10 bits, the softening points of both PCF and SMF were reached slightly differently, therefore, there was a lower loss of MFD due to the mismatch between MFDs of both PCF and SMF which is the result of an expanding mode in the collapsed region.

5. Conclusion

In this paper, we have reported the relationship between splice losses and air holes collapse length when splicing (SMF-PCF) of the same MFD at arc powers of STD –10, STD 00, and STD +10 bits, while the arc time was varied from 500 to 3000 ms. It has been observed that the lower splice loss is achieved at STD +10 bits (see Fig. 10) and that the minimum air holes collapse length is achieved at STD –10 bits. The relationship between splice loss and collapse length was almost linear. This study may find applications in the design of PCF and development of optical communication.

References

[1] KHATUN M.R., ISLAM M.S., BAZLUR RASHID A.N.M., *Analysis of dual core hexagonal PCF based polarization beam splitter*, Computer Engineering and Intelligent Systems **3**(3), 2012, pp. 1–9.

[2] KUMAR P., SHARAM K.K., KANUNGO V., *Some PCF structures with elliptical air holes bansed on Dolph Tschebysheff polynomials and its propagation characteristics*, International Journal of Engineering Research and Applications (IJERA) **2**(3), 2012, pp. 2689–2694.

[3] REVATHI S., INABATHINI S., SANDEEP R., *Soft glass spiral photonic crystal fiber for large nonlinearity and high birefringence*, Optica Applicata **45**(1), 2015, pp. 15–24.

[4] CHACKO S.C., CHERIAN J.M., SUNILKUMAR K., *Low confinement loss photonic crystal fiber (PCF) with flat dispersion over C-band*, International Journal of Computer Applications **85**(15), 2014, pp. 5–7.

[5] SHAYMAA N. ISMAIL, HANAN. J. TAHER, AL-JANABI A.H., *Fusion splicing for a large mode area photonic crystal fiber with conventional single mode fiber*, Iraqi Journal of Laser **13**(A), 2014, pp. 9–17.

[6] LIMIN XIAO, DEMOKAN M.S., WEI JIN, YIPING WANG, CHUN-LIU ZHAO, *Fusion splicing photonic crystal fibers and conventional single mode fibers: microhole collapse effect*, Journal of Lightwave Technology **25**(11), 2007, pp. 3563–3574.

[7] KUMAR A., CHHABRA K., SETHI L., *Injected micro structured fabricated optical fibers with a standard fusion splicer*, International Journals of Research (IJR) **1**(10), 2014, pp. 978–984.

[8] YABLON A.D., BISE R.T., *Low-loss high-strength microstructured fiber fusion splices using GRIN fiber lenses*, IEEE Photonics Technology Letters **17**(1), 2005, pp. 118–120.

[9] MEHDE M.S., SALAH ALDEEN ADNAN TAHA, AMMAR ANWER AHMED, *The optimum conditions for arc fusion to splice photonic crystal fiber and single mode optical fiber*, Engineering and Technology Journal **33**(1), 2015, pp. 101–113.

[10] MASSARO A., *Photonic Crystals – Introduction, Applications and Theory*, 1st Ed., InTech Publication, 2012, Chapter 9, pp. 185–187.

[11] PRIYAMBADA S., SINGH D.K., *Analysis of effective area and splicing loss behavior of square and hexagonal photonic crystal fiber*, International Journal of Scientific and Research Publications **3**(5), 2013, pp. 1–4.

[12] VILLATORO J., MINKOVICH V.P., PRUNERI V., BADENES G., *Simple all-microstructured-optical-fiber interferometer built via fusion splicing*, Optics Express **15**(4), 2007, pp. 1491–1496.

[13] MYOUNG JIN KIM, KWAN SEOB PARK, HAE YOUNG CHOI, SE-JONG BAIK, KIEGON IM, BYEONG HA LEE, *High temperature sensor based on a photonic crystal fiber interferometer*, Proceedings of SPIE **7004**, 2008, article 700407.

[14] Thorlabs ESM-12B Photonic Crystal Fiber Data Sheet, https://www.thorlabs.com/thorcat/22700/ESM-12B-SpecSheet.pdf

[15] BENNETT P.J., MONRO T.M., RICHARDSON D.J., *Toward practical holey fiber technology: fabrication, splicing, modeling, and characterization*, Optics Letters **24**(17), 1999, pp. 1203–1205.

Received June 19, 2015
in revised form October 6, 2015